INDIAN JOURNAL OF SCIENCE AND TECHNOLOGY

RESEARCH ARTICLE

Differentiating Stagnant Water from Wet Surface for Detecting Potential Mosquito Breeding Sites in Real Time

Sonali Bhutad[1], Kailas Patil[1]*, Nishad Khare[2]

1 Department of Computer and Technology, Vishwakarma University, Pune, India
2 Department of Computer Engineering, Pune Vidyarthi Griha's College of Engineering and Technology, Pune, India

OPEN ACCESS

Received: 31-10-2022
Accepted: 14-12-2022
Published: 04-02-2023

Citation: Bhutad S, Patil K, Khare N (2023) Differentiating Stagnant Water from Wet Surface for Detecting Potential Mosquito Breeding Sites in Real Time. Indian Journal of Science and Technology 16(5): 331-338. https://doi.org/10.17485/IJST/v16i5.2111

* **Corresponding author**.

kailas.patil@vupune.ac.in

Funding: None

Competing Interests: None

Published By Indian Society for Education and Environment (iSee)

ISSN
Print: 0974-6846
Electronic: 0974-5645

Abstract

Objective: Mosquito breeding site detection is crucial due to the colorization of water. Most systems fail to identify different types of stagnant water; hence, accurate water identification is essential. This study aims to devise an approach that can help increase the accuracy of detecting and distinguishing stagnant water from that of other wet surfaces. **Methods:** This work has proposed a technique using anchor boxes to reduce misclassification for detecting stagnant water. The images were collected for different types of water. The dataset was manually created by labeling images. **Findings:** We evaluated the proposed approach's results and discovered that changing the anchor size and increasing training iterations on the dataset reduced misclassification by 89.20%. **Novelty:** The proposed method improves accuracy by using suitable anchor boxes to distinguish the water body from the wet surface. Unlike existing systems that are only capable of detecting a particular type of water; the improved YOLO V3 detects wet surfaces and different types of stagnant water due to training on a real-time customized dataset.

Keywords: Object detection; Stagnant water; Street-View images; Misclassification; Mosquito breeding site

1 Introduction

The existing research papers detect mosquito breeding sites according to container types. Hence, it is not possible to perform detections for all water types. To fill this gap, we have created a unique dataset for experimentation. For mosquito breeding site detection, it was required to identify the presence of stagnant water. Stagnant water in an ignored site for a longer duration may develop mosquito larvae in it [(1)]. This attribute, i.e., stagnant or remaining water, helps identify the possible mosquito breeding hotspots. Further analysis of the images of stagnant water revealed that the usual coloration of the water retention areas may misclassify the data.

The need for the performance of YOLO V3 is discussed in the research papers, but misclassification is not considered [(2)]. Misclassification is wrongly assigning an object to a different category. Every approach detects water based on a specific attribute

that may misclassify the data, e.g., in [2] the author was detecting only water tanks. Thus, detecting other types of water like muddy or transparent water is impossible. In different deep learning approaches, as in [3], water identification was done using a Densenet on satellite images. Here the author says that a Densenet cannot identify all the water areas but can precisely distinguish between water and land areas. In [4], water detection is done for container types only; hence it is not possible to detect various forms of the water bodies. Though many object detection techniques exist for geospatial object detection [5,6], they just detect the water presence and not the boundary of the stagnant water. Whereas object detection based on infrared images detects surface water with boundary [7] but increases the cost. The need for mechanisms for pollutant and non-pollutant stagnant water detection is clearly mentioned in the existing papers related to potential mosquito breeding habitats [8]; as none of the existing mechanisms detect mosquito breeding sites based on the water surface from lower altitudes. This paper proposes a low-cost approach with street-view images for detecting different water forms to address the limitations mentioned above. In addition to that, we are detecting not only stagnant water but wet surface around it which makes this work novel. Therefore, a real-time object detection algorithm YOLO V3 was chosen due to its good accuracy and speed [9]. In this research, we had success in detecting various forms of water like muddy, transparent, blue, green, and black water. The main contributions of this work are summarized below,

1. We are identifying the boundary of stagnant water from lower altitudes using street-view images. Which is necessary for pesticide spraying for infectious disease management. Furthermore, if spraying is done according to the boundary of the stagnant water then it will help save pesticide usage and will contribute to the future applications of the Sustainable Development Goal -6 of the United Nations, i.e., "water and sanitation" (UN SDG -6) [10].
2. We proved that a change in anchor size reduces misclassification in object detection which increases the accuracy of the stagnant water detection. The suitable anchors were calculated using the K-means algorithm and a label smoothing technique.
3. Due to the unavailability of a stagnant water dataset, a unique dataset of 1976-labeled stagnant water images was created and published in the Mendeley Repository wherein all the adversarial conditions were considered beforehand to create labels for the dataset images.

The comparative analysis of the existing method is done with our method and the results are shown in Table 1,

Table 1. Comparative Analysis of Detection Criteria

Mosquito Breeding Site Detection Criteria					
Author Name	**Object**	**Water Type**	**Images**	**Real-Time Detection**	**Differentiating Water From the Surrounding area**
Jared Schenkel [1]	Plastic bottle, Glass bottle, plastic lid, Bucket, Cup, Bag Can	Nil	UAV images with GPS coordinates	No	No
Daniel Trevisan Bravo [2]	Water Tank	Nil	UAV images	No	No
Passos [4]	Bottle, Pool, Bucket, Tire, Puddle, Water tank	Nil	Aerial images	Yes	No
Peter Haddawy [11]	Potted plant, Tire, Jar, Bin, Ceramic Bowl	Nil	Street View	No	No
Proposed System	All containers and Surface water	Black, Green, Muddy, Blue, Shiny	Street View	Yes	Yes

2 Methodology

2.1 Dataset creation and collection

When standing water is left unclean and unattended for a long time, it leads to water stagnation. Water stagnation could be seen after rains. Rainwater gets collected in potholes, open tubs, and blocked drains. Other places where water can stagnate are old cans, tires, roofs, hollows of trees, open containers, etc. Based on the above cases, a dataset was created by considering the

probable misclassification in the case of water detection, which may occur in the cases shown in Table 3. For the dataset of 3812 images, the sources used and the number of images captured were given in Table 2. Tong et al.[12] thought that "information fusion is the study of efficient methods for automatically or semi-automatically transforming information from different sources and points in time into a representation that provides effective support for human or automated decision making." Thus, to increase object detection performance, data fusion was done by adding google images with real-time images[12].

Table 2. Dataset Sources

Training Set			**Test Set**
Google Chrome	Android phone	Rotated by 90 degrees	Google Chrome
1200	1976	100	536

Images were resized to 256 X 256 dimensions, and two classes, namely water, and wet surface were taken. The class name wet surface was used to recognize different parts of images such as wet-earth surface, wet-road surface, wet tiles, and mud. In contrast, the water class recognizes different types of water, such as muddy, black water, blue water, shiny water, and green water. A ground truth box in an image shows the position of an object in the entire image. Manually ground truth boxes were drawn using the LabelImg tool. This tool was used to uniformly label each water/wet surface on the pictures of the training set and test set, and a text file corresponding to the pictures was generated for the network training. The resultant dataset is published in Mendeley Repository[10].

The actual labeling steps are as below,

1. Select and frame the water/wet area using the mouse;
2. Double-click to mark the corresponding label category;
3. Click Save after marking.

As shown in Figure 1, for 2D dataset creation the strategy mentioned in[11] was used for image annotation. The YOLO V3 algorithm accepts the coordinates in the following format,

Class X-min Y-min width height

Where class is the object class, (X-min, Y-min) are center coordinates of the bounding box and width, height represents the width and height of the bounding box

Table 3. Probable Misclassification

Similar object	**Type of water**
Mud	Muddy water
Tar Road	Blackwater
Wet pothole	Blackwater
Wet earth surface	Muddy water

2.2 Water Detection Process of YOLO V3

Various boxes were predicted at different scales using the concept of a feature pyramid network. It mainly utilizes residual layers and a certain number of convolutional layers to complete the detection process and uses the entire image features to predict each bounding box. At the same time, it predicts all classes of all bounding boxes for the complete training, which maintains maximum average accuracy and strong real-time performance[13]. As shown in Figure 1, it divides the input image into N×N grids and assigns one anchor bounding box for each ground truth object. Equations 2-5 show four coordinates (tx, ty, tw, th) predicted by the network for each bounding box, and then a function was used to predict three corresponding parameters in the form of coordinates like the center point coordinates (cx, cy) of the bounding box, the width- bw, and the height- bh[14]. Where σ (•) is the sigmoid activation function, which was used to limit the center like the center point coordinates (bx, by) of the bounding box, the width bw, and the height bh. The confidence in the detected object was calculated by the formula given below,

$$\text{Object confidence} = \text{Prediction}(\text{object}) \times IOU^{\text{tuth pred}} \quad (1)$$

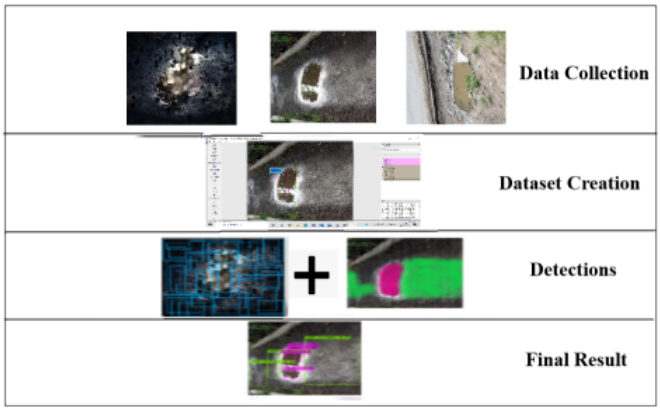

Fig 1. General Approach of YOLO V3

The prediction of the bounding box and the Intersection-over-Union (IOU) were shown in Figure 1,using the following equations[15].

$$bx = \sigma(tx) + cx \tag{2}$$

$$\mathrm{by} = \sigma(\mathrm{ty}) + \mathrm{cy} \tag{3}$$

$$\mathrm{bw} = \mathrm{p_w e^{tw}} \tag{4}$$

$$\mathrm{bh} = \mathrm{p_h e^{th}} \tag{5}$$

Where the IOU in equation (1) is the overlapping rate between the bounding box detected by the system and the ground truth.

2.3 Transfer learning

The method in which a deep learning model developed for one task is reused as the parameter initialization for another model on a different task is called transfer learning. One of the advantages of transfer learning is that a network trained with a small ground-truth dataset can also reach a high detection accuracy. Therefore, transfer learning from Darknet-53 for the YOLO V3 framework was carried out. We applied transfer learning using YOLO V3 weights to initialize our training. YOLO V3 has 106 convolutional layers and could detect a variety of different classes ranging from cats to cars, but it did not detect water. Therefore, a custom dataset was created for water detection. For training, the backbone network Darknet-53 was used, and two classes, namely water, and wet surface were taken. The YOLO V3 model was trained and tested on Google Colab with 45,000 iterations.

Table 4. Result for Different Sets of Anchors

Anchors	MAP	TP	FP	FN	Precision	Recall	Time	IoU avg
Version 1	85.67	51469	13701	9879	0.79	0.84	39 seconds	58.08 %
Version 2	87.24	51692	12625	9656	0.80	0.84	39 seconds	59.76%
Version 3	89.20	52469	11658	8440	0.82	0.86	38 seconds	61.81 %

3 Results and Discussion

For testing, the platform used was a desktop computer with an Intel i5 1035G1 (1.19 GHz) dual-core CPU, a GeForce MX250, 2GB GPU (384 CUDA cores), and 8 GB of memory, running on a Windows 10, 64-bit system. The software tools used included CUDA 10.2, CUDNN 5.0, OpenCV3.0, and Microsoft Visual Studio 2019. To verify the effectiveness of the detection, the test data set of google images was used. Further, we analyzed the experimental data and compared the results. Detection results are shown in Figures 2 and 3.

All the recent work has been done on mosquito breeding site detection based on container types. Hence a direct comparison is not available for our work. The existing approaches are not suitable for different types of water surfaces and hence cannot be generalized for all types of potential mosquito breeding site detection. To make mosquito breeding site detection generalized, it was required to perform detection according to stagnant water surface [2] and not as per the container type. In [3], a novel approach with the combination of the enhanced super-pixel method and CNN was used for waterbody extraction from high-resolution remote sensing images. Here the author was successful in distinguishing between the water pixel and the shadow pixel. The water body extraction from Landsat Imagery was done using a stacked sparse autoencoder and a feature expansion algorithm. In [4], the author has considered different containers which work for a particular type of container only. According to the author, this approach gives high accuracy on limited training samples, but misclassification [10] in water is not considered. In [16], a solution was proposed to increase the object detection accuracy of YOLO V3 for UAV images by combining lower feature maps with bounding box regression and data augmentation where the user has reduced the false detections of YOLO V3. As the wet surface is usually around the boundary of water and due to limitations of YOLO V3 [17], misclassification may happen; hence wet surface labeling of the dataset was done. However, none of the existing papers considered detection for different water types.

We first explore stagnant water detection for different water surfaces with misclassification reduction by modifying anchors. As the problems of missed detection and false detection happened in the monitoring process of water detection, hence for experimentation, MAP, Precision, and Recall were used as evaluation parameters. The precision was the ratio of the number of correctly detected water/wet areas to the total number of detected water/wet areas. The Recall was the ratio of the number of correctly detected water/wet areas to the total number of water/wet in the data set. The calculation method is shown in equations (7) and (8).

$$\text{Precision} = \frac{\text{TP}}{\text{TP}+\text{FP}} \tag{7}$$

$$\text{Recall} = \frac{\text{TP}}{\text{TP}+\text{FN}} \tag{8}$$

In these formulas, True Positive (TP) indicates the number of correctly detected water/wet surfaces, True Negative (TN) indicates the number of correctly detected backgrounds, False Positive (FP) indicates the number of incorrect detections, and False Negative (FN) indicates the number of missed detections, respectively. The MAP is the average of AP (average precision), and AP is the average of all categories, i.e., classes used for labeling. The mean average precision is calculated by taking an average of precision for several recall values. To reduce misclassification, the anchor size was changed, and iterations were increased. The anchor box plays a major role in the localization of the object because the center coordinates of the anchor box decide the position of the object. Then the distance of the object center (cx,cy) concerning the grid was used to calculate (bx, by, bw, bh). Each version of the anchor box shown in Table 5 gave different accuracy and false positives as shown in Table 4. Out of the three versions, the last version provided MAP with 89.20 %, Recall with 0.86, and Precision 0.82. In [2], YOLOV3 performance for water container detection is 90 %, but in the future scope, the need for stagnant water detection is mentioned.

Table 5. Set of Anchors

Versions	Anchors
Version-1	22,17, 23, 27, 27, 40, 37, 58, 52, 27, 43, 76, 86, 52, 105, 115, 135,169
Version-2	17,12, 21, 27, 40, 20, 30, 53, 63, 35, 50, 73, 105, 60, 69,125, 153, 114
Version-3	16, 13, 33, 19, 21, 36, 40, 43, 66, 27, 40,83, 86, 56, 73,122, 151, 102

The corresponding detection results for muddy and black water were shown in Figures 2 and 3, respectively. The trained YOLO V3 could also detect other types of water like blue water, green water, and transparent water. This work is unique because no other existing system could detect water on wet surfaces in real time using YOLO V3 in street view images.

3.1 Image size 416x416

While doing experimentation, we tried training with image size 416X416 by changing a parameter in the configuration file as suggested in [18,19]. However, it caused too much overfitting in the detection results. Therefore, YOLO V3 is trained on an image size of 256 pixels.

3.2 Performance comparison

When the dataset was applied on YoloV4-tiny for comparing accuracy. The anchor set used for YoloV4-tiny contained 6 pairs which were 22, 17, 27, 40, 52, 27, 43, 76, 86, 52, 105,115. We found that YOLO V3 is way more accurate and suitable for water detection due to its accuracy and speed. In terms of object detection, false positives (FP) were very less than True Positives (TP), so the chances of misclassification were less. Due to less number of convolution layers, the training time of YoloV4-tiny was less as compared to YOLO V3, but accuracy was very poor. The results achieved in terms of MAP and other parameters are shown in Table 6. Therefore, YOLO V3 performs better to detect the presence of water, than YOLO V4-tiny. Further, we improved YOLO V3 by modifying anchors that have given an accuracy MAP of 89.20 %. Thus, the improved YOLO V3 is more accurate than the original YOLO V3.

Table 6. YOLO V3 and YOLO V4-tiny Accuracy Comparison

Algorithm	MAP	TP	FP	FN	Precision	Recall	Time	IoU avg
YOLO V3	75.67	45573	19309	15775	0.70	0.74	40 seconds	50.00 %
Improved YOLO V3	89.20	52469	11658	8440	0.82	0.86	38 seconds	61.81 %
YoloV4-tiny	34.48	29163	53783	32165	0.35	0.48	44 seconds	22.71%

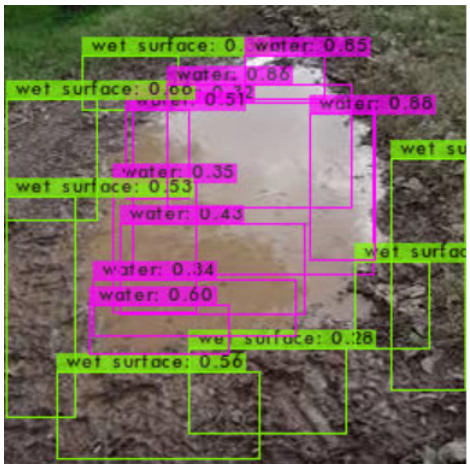

Fig 2. Water and Wet Surface Detection (Muddy water)

Fig 3. Water and Wet Surface Detection (Blackwater)

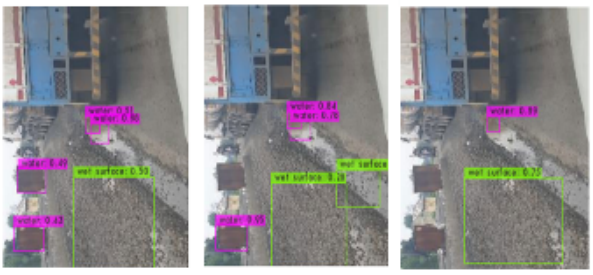

Version-1 Misclassification Figure-4.

Version-2 Misclassification Figure-5.

Version-3 No Misclassification Figure-6.

4 Conclusion

This study dwells on a mechanism to identify potential mosquito breeding sites in real-time using stagnant water surface detection. The experimentation done on YOLO V3 using anchor boxes shows that misclassification can be reduced by using suitable anchors. From the results achieved it is clear that this work distinguishes water bodies from wet surfaces effectively. Thus, we explored the use of YOLO V3 for different anchor sets to reduce misclassification for different water types. Using the best-suited anchor set, we could achieve an MAP of 89.20%. As in some cases of shiny water, misclassification is still there, hence future work will be based on removing misclassification based on the texture of images detecting stagnant water accurately. This research is novel as we concentrated on the color of stagnant water and the wet surface around it, which accurately distinguishes different stagnant water surfaces from the wet surface using modified anchors. The existing approaches are not suitable for different types of water surfaces and hence cannot be generalized for all types of potential mosquito breeding site detection. Our mechanism helps detect potential mosquito breeding sites in agricultural and urban areas up to 93 % except for shiny water surfaces, which is around 83%. Thus, this research could be utilized in a low-cost system for detecting mosquito breeding sites formed due to muddy, black water, green water, and blue water.

References

1) Schenkel J, Taele P, Goldberg D, Horney J, Hammond T. Identifying Potential Mosquito Breeding Grounds: Assessing the Efficiency of UAV Technology in Public Health. *Robotics*. 2020;9(4):1–12. Available from: https://doi.org/10.3390/robotics9040091.
2) Bravo GADT, Lima WAL, Alves V, Colombo LP, Djogbenou. Sergio Vicente Denser Pamboukian, Cristiano Capellani Quaresma, Sidnei Alves de Araujo.Automatic detection of potential mosquito breeding sites from aerial images acquired by unmanned aerial vehicles. *Computers, Environment and Urban System*. 2021;90:1–13. Available from: https://doi.org/10.1016/j.compenvurbsys.2021.101692.
3) Wang G, Wu M, Wei X, Song H. Water Identification from High-Resolution Remote Sensing Images Based on Multidimensional Densely Connected Convolutional Neural Networks. *Remote Sensing*. 2020;12(5):1–20. Available from: https://doi.org/10.3390/rs12050795.
4) Passos WL, Araujo GM, De Lima AA, Netto SL, Silva EABD. Automatic detection of Aedes aegypti breeding grounds based on deep networks with spatio-temporal consistency. *Computers, Environment and Urban Systems*. 2022;93(101754). Available from: https://doi.org/10.48550/arXiv.2007.14863.
5) Wu X, Hong D, Chanussot J, Xu Y, Tao R, Wang Y. Fourier-Based Rotation-Invariant Feature Boosting: An Efficient Framework for Geospatial Object Detection. *IEEE Geoscience and Remote Sensing Letters*. 2020;17(2):302–306. Available from: https://doi.org/10.1109/LGRS.2019.2919755.
6) Hong D, Gao L, Yao J, Zhang B, Plaza AJ, Chanussot J. Graph Convolutional Networks for Hyperspectral Image Classification. *IEEE Transactions on Geoscience and Remote Sensing*. 2021;59(7):1–13. Available from: https://doi.org/10.1109/TGRS.2020.3015157.
7) Wu X, Hong D, Huang Z, Chanussot J. Infrared Small Object Detection Using Deep Interactive U-Net. *IEEE Geoscience and Remote Sensing Letters*. 2022;19:1–5. Available from: https://doi.org/10.1109/LGRS.2022.3218688.

8) Mathania MM, Munisi DZ, Silayo RS. Spatial and temporal distribution of Anopheles mosquito's larvae and its determinants in two urban sites in Tanzania with different malaria transmission levels. *Parasite Epidemiology and Control*. 2020;11(e00179). Available from: https://doi.org/10.1016/j.parepi.2020.e00179.
9) Padmanabula SS, Puvvada RC, Sistla V, Kolli VKK. Object Detection Using Stacked YOLOv3. *Ingénierie des Systèmes d'Information* . 2020;25(5):691–697. Available from: https://doi.org/10.18280/isi.250517.
10) Bhutad S, Patil K. Dataset of Stagnant Water and Wet Surface Label Images for Detection. *Data in Brief*. 2022;40(107752). Available from: https://doi.org/10.1016/j.dib.2021.107752.
11) Haddawy P, Wettayakorn P, Nonthaleerak B, Yin MS, Wiratsudakul A, Schöning J, et al. Large scale detailed mapping of dengue vector breeding sites using street view images. *PLOS Neglected Tropical Diseases*. 2019;13(7):e0007555–e0007555.
12) Tong M, Xuyang J, Zheng Y, Witold C. A survey on machine learning for data fusion. *Information Fusion*. 2020;57:115–129. Available from: https://doi.org/10.1016/j.inffus.2019.12.001.
13) Alcorn MA, Li Q, Gong Z, Wang C, Mai L, Ku WS, et al. Strike (With) a Pose: Neural Networks Are Easily Fooled by Strange Poses of Familiar Objects. *2019 IEEE/CVF Conference on Computer Vision and Pattern Recognition (CVPR)*. 2019.
14) Gea J, A DZ, Yanga L. Road sludge detection and identification based on improved YOLO V3. *6th International Conference on Systems and Informatics*. 2019;p. 1–5.
15) Chen H, He Z, Shi B, Zhong T. Research on Recognition Method of Electrical Components Based on YOLO V3. *IEEE Access*. 2019;7:157818–157829.
16) Xing C, Liang X, Ma Y. A Solution to Improve Object Detection for Images Captured by UAV-mounted Camera. *2019 IEEE 7th International Conference on Computer Science and Network Technology (ICCSNT)*. 2019. Available from: https://ieeexplore.ieee.org/stamp/stamp.jsp?arnumber=8962431.
17) Minaee S, Boykov YY, Porikli F, Plaza AJ, Kehtarnavaz N, Terzopoulos D. Image Segmentation Using Deep Learning: A Survey. *IEEE Transactions on Pattern Analysis and Machine Intelligence*. 2021;p. 1–20. Available from: https://doi.org/10.1109/TPAMI.2021.3059968.
18) Menghan Z, Zitian L, Yuncheng S. Optimization and Comparative Analysis of YOLOV3 Target Detection Method Based on Lightweight Network Structure. *2020 IEEE International Conference on Artificial Intelligence and Computer Applications (ICAICA)*. 2020;p. 1–5. Available from: https;//doi.org/10.1109/ICAICA50127.2020.
19) Huang YQ, Zheng JC. Optimized YOLOv3 Algorithm and Its Application in Traffic Flow Detections. *Applied Sciences*. 2020;10(9):3079. Available from: https://www.mdpi.com/2076-3417/10/9/3079.